



**HAL**  
open science

## Tracer Dispersion in Rough Open Cracks

Stéphane Roux, Franck Plouraboué, Jean-Pierre Hulin

► **To cite this version:**

Stéphane Roux, Franck Plouraboué, Jean-Pierre Hulin. Tracer Dispersion in Rough Open Cracks. Transport in Porous Media, 1998, 32 (1), pp.97-116. 10.1023/A:1006553902753 . hal-03607677

**HAL Id: hal-03607677**

**<https://hal.science/hal-03607677>**

Submitted on 14 Mar 2022

**HAL** is a multi-disciplinary open access archive for the deposit and dissemination of scientific research documents, whether they are published or not. The documents may come from teaching and research institutions in France or abroad, or from public or private research centers.

L'archive ouverte pluridisciplinaire **HAL**, est destinée au dépôt et à la diffusion de documents scientifiques de niveau recherche, publiés ou non, émanant des établissements d'enseignement et de recherche français ou étrangers, des laboratoires publics ou privés.

# Tracer Dispersion in Rough Open Cracks

STÉPHANE ROUX<sup>1</sup>, FRANCK PLOURABOUÉ<sup>2</sup> and JEAN-PIERRE HULIN<sup>3</sup>

<sup>1</sup>*Surface du Verre et Interfaces, UMR CNRS/St-Gobain n° 125, 39 Quai Lucien Lefranc, F-93303 Aubervilliers Cedex, France*

<sup>2</sup>*Institut de Mécanique des Fluides, UMR CNRS n° 5502, Allée du Pr. C. Soula, 31400 Toulouse, France*

<sup>3</sup>*Laboratoire Fluide, Automatique et Systèmes Thermiques, URA CNRS n° 871, Bât. 502, Univ. Paris-Sud, 91405 Orsay Cedex, France*

**Abstract.** Tracer dispersion is studied in an open crack where the two rough crack faces have been translated with respect to each other. The different dispersion regimes encountered in rough-wall Hele-Shaw cell are first introduced, and the geometric dispersion regime in the case of self-affine crack surfaces is treated in detail through perturbation analysis. It is shown that a line of tracer is progressively wrinkled into a self-affine curve with an exponent equal to that of the crack surface. This leads to a *global* dispersion coefficient which depends on the distance from the tracer inlet, but which is still proportional to the mean advection velocity. Besides, the tracer front is subjected to a *local* dispersion (as could be revealed by point measurements or echo experiments) very different from the global one. The expression of this anomalous local dispersion coefficient is also obtained.

**Key words:** dispersion, anomalous diffusion, Taylor dispersion, roughness, self-affine.

## 1. Introduction

Tracer dispersion in flows between parallel rough walls displays an amazingly rich variety of scaling regimes. Even in a perfect Hele-Shaw cell (parallel plate geometry with a simple plane Poiseuille flow), the vanishing of the fluid velocity at the wall induces a large dispersion at high Péclet numbers, as shown theoretically by Taylor [1, 2]. Taking into account aperture fluctuations in a Hele-Shaw cell gives rise to several different regimes, each of them being characterized by a specific scaling of the dispersion coefficient with the Péclet number. The roughness of the walls of the Hele-Shaw cell have been shown to play a significant role in dispersion, experimentally and numerically [3–6], in particular at low velocity. The aim of the present study is to analyze the peculiar dispersion behavior induced by the multiplicity of length scales of the crack surface roughness observed experimentally. Indeed, it has been shown that a self-affine behavior provided an accurate statistical description of the topography of crack surfaces. In a typical fault, the two walls bounding the flow are ‘conjugated’, and can be matched by a mere translation. The aperture field can thus be simply characterized by a few physical parameters. Such a case is referred to as a model for rock ‘joints’. It will be shown that one of the many regimes encountered in dispersion is strongly affected by such a crack geometry, and results in interesting size effects.

The paper is organized as follows. In the second section, the different regimes classically encountered in Hele-Shaw flow with an imperfect geometry are quickly reviewed using scaling arguments. However, only the case of a single scale of heterogeneity will be considered and aperture fluctuations above this scale will be assumed to be decorrelated. The cross-over scales are discussed in terms of the Péclet number constructed on the mean aperture. In the third section, the dispersion in a joint model in the so-called ‘geometric dispersion regime’ is analyzed. This regime is the most important one in practice. The dispersion coefficient describes the wrinkling of the initially straight tracer line, which is shown to develop progressively a self-affine geometry with an upper scale cut-off proportional to the traveled distance. Finally, in the fourth section, the intrinsic widening of the tracer line is discussed. The latter can be measured from point measurements of the dispersion process. The conclusion summarizes the main results obtained.

## 2. Different Dispersion Regimes in an Imperfect Hele-Shaw Cell

Tracer dispersion in a Hele-Shaw flow displays an interesting scaling effect with the flow velocity which has been first theoretically analyzed by Taylor [1]. Although this case can be solved exactly, a simple scaling argument is proposed which provides the correct answer up to numerical factors. The discussion will be extended to the case of inhomogeneous flow. The aim is here, more to clarify the different scaling regimes than to provide exact estimates. Therefore, in the sequel, all pure numbers which come as prefactors are omitted. Thus, the equality signs appearing in the following subsection are implicitly to be understood as ‘proportional to’. It should, however, be underlined that prefactors may play an important role in practice. For instance, in the case of Taylor dispersion to be detailed below, the following exact result can be established [7]:

$$D = \frac{1}{210} \frac{U^2 h^2}{D_m} + D_m, \quad (1)$$

where  $U$  is the mean advective velocity,  $h$  the aperture,  $D_m$  the molecular diffusion coefficient. In the scaling arguments, the pure number  $1/210$  is treated as 1! The important message here is to retain the dependence of the dispersion coefficient on crucial parameters, such as mean and standard deviation of velocity, molecular diffusion coefficients, correlation lengths, etc.

### 2.1. TAYLOR DISPERSION

Let us consider a Hele-Shaw cell of aperture  $h$ , in which a uniform Poiseuille flow is established along the  $x$  direction. The mean velocity along the  $x$ -axis is called  $U$  so that the velocity across the height  $z$  is written

$$u(z) = (3U/2)(1 - 4z^2/h^2) . \quad (2)$$

Let us introduce  $D_m$  the molecular diffusion coefficient of the tracer. The reason for the anomalous dispersion is due to the vanishing of the velocity near the wall, leading to a divergent advection time in the absence of diffusion.

To clarify this point, it is useful to consider the following limit of infinite Péclet number (i.e.  $D_m = 0$  or pure advection). A tracer particle launched at the origin (in particular, in the middle plane of the cell) will be convected over a distance  $L$  in a time  $T(0) = 2L/3U$ . If the particle is launched for a point at a distance  $z$  above the origin, the time needed to be convected by the same distance is  $T(z) = T(0)(1 - 4z^2/h^2)^{-1}$ . Therefore, for a uniform distribution of tracer across the cell height, the transit time distribution for a distance  $L$  will be a power-law decaying in time as  $p(T) \propto T^{-2}$ . When  $D_m$  is zero,  $p(T)$  has thus an infinite variance and, therefore, the dispersion coefficient is infinite. However, as soon as  $D_m$  is nonzero, the time distribution acquires a natural cut-off given by the time needed for a particle to diffuse away from the wall. This truncation time  $\tau$  is a diffusion time over a characteristic distance  $h$ , i.e.

$$\tau = \frac{h^2}{D_m}. \quad (3)$$

Within the time  $\tau$  needed to escape from the wall, a tracer located close to the center of the cell will travel over a distance proportional to  $\Delta x = U\tau$ . Introducing the dispersion coefficient  $D$ , which describes the spreading of the tracer for large times,  $t$ , as a distance proportional to  $\sqrt{Dt}$ , it suffices to apply this relation at the largest (limiting) time encountered in the process,  $\tau$ , above which no correlation is preserved on the tracer trajectory, and thus, dispersion is normal and  $D$  assumes a constant value. Hence,  $D\tau = \Delta x^2$  or

$$D = U^2\tau = \frac{U^2h^2}{D_m}. \quad (4)$$

Introducing the Péclet number  $Pe \equiv Uh/D_m$  over the scale  $h$ , the so-called ‘Taylor’ regime (label ‘T’) is obtained

$$\frac{D}{D_m} = Pe^2. \quad (5)$$

In the previous argument a uniform distribution of tracer across the aperture was considered. It should be pointed out, however, that other boundary conditions may be more appropriate to model an actual dispersion experiment.

This description in fact applies for  $Pe \gg 1$ . For lower Péclet numbers, molecular diffusion gives a larger spreading so that  $D \approx D_m$  at small velocities. The scaling regimes can be summarised as

$$\frac{D}{D_m} = \begin{cases} \mathcal{O}(Pe^0) & \text{for } Uh/D_m \ll 1, \\ \mathcal{O}(Pe^2) & \text{for } Uh/D_m \gg 1. \end{cases} \quad (6)$$

## 2.2. GEOMETRICAL DISPERSION

Let us now introduce some inhomogeneities in the flow. The aperture of the Hele-Shaw cell is now modulated randomly with a correlation function of the aperture, which decays over a characteristic length scale  $\xi$ . The effect of anisotropy will be discussed in a following section. For the present discussion,  $\xi$  denotes essentially a correlation length for the velocity along the flow direction, and thus is written a subscript  $\xi_{\parallel}$ . Only small departures from the Hele-Shaw geometry will be considered so that, locally, a Poiseuille flow across the thickness is preserved. This so-called Reynolds approximation implies that the cell aperture fluctuations are locally small in magnitude and the modulations of cell thickness occur at large wavelengths compared to  $h$ . Such a geometry leads to small relative fluctuations of the aperture field  $\delta h/h \ll 1$  which is similar to a weak disorder permeability field approximation [8, 9]. A second condition is mandatory for the geometrical dispersion regime to occur. The velocity correlation length must be larger than the mean aperture:  $\xi_{\parallel} \gg h$ . In practice, the second requirement is the most restrictive.

The aperture fluctuations give rise to velocity fluctuations called  $\delta U$ . It should be understood that the Stokes flow hypothesis implies that  $\delta U$  is proportional to  $U$ . Therefore, a dimensionless parameter  $\varepsilon = (\delta U)/U$  is introduced which is independent of the Péclet number. A simple perturbation calculation shows as in [8] that to leading order,  $\varepsilon$  is proportional to the relative aperture fluctuation. Those inhomogeneities in the flow modify the dispersion coefficient for intermediate Péclet numbers, but the two extreme behaviors (molecular diffusion and Taylor dispersion) remain unaffected. Let us first consider tracer particles confined in the mean plane of the cell. The inhomogeneity of the flow will induce a spreading of tracer transit times over the characteristic length scale  $\xi_{\parallel}$  of order  $\Delta T \propto \xi_{\parallel}(\delta U)/U^2$  so that the estimated dispersion coefficient amounts to  $D = \xi_{\parallel}\varepsilon^2 U$ . The scaling of the dispersion coefficient in this regime is thus

$$\frac{D}{D_m} = \varepsilon^2 \frac{\xi_{\parallel} U}{D_m} = \varepsilon^2 \frac{\xi_{\parallel}}{h} \text{Pe}, \quad (7)$$

implying a simple proportionality between  $D$  and the mean flow velocity. This linear scaling of  $D$  vs.  $U$  is often called *geometrical dispersion*, (labeled ‘G’ in the sequel) in the sense that  $D$  is independent of the molecular diffusion coefficient, and merely controlled by the inhomogeneity of the flow. It is however important to note that even if  $D_m$  does not contribute to the expression of  $D$ , it nevertheless dictates the upper and lower bounds for the validity of this regime. It must be underlined that this geometrical dispersion regime is the most relevant one for practical applications, in particular for crack flow [6].

In order to account for the Taylor regime, it suffices to perform a simple convolution of the exit time distribution by a  $t^{-2}$  kernel truncated at the diffusion time  $\tau$  (Equation (3)) as for the case of a simple Hele-Shaw cell explicitied above. As a result, the total dispersion coefficient will appear to be the sum of the above derived dispersion coefficient plus the one due to Taylor dispersion. Balancing those two

terms, a cross-over is observed from geometrical to Taylor dispersion at a Péclet number equal to

$$\text{Pe}_{\text{GT}} = \frac{\xi_{\parallel} \varepsilon^2}{h}. \quad (8)$$

Below, it will be shown that the transverse diffusion may give rise to yet another ‘anomalous’ dispersion regime. If the latter is not present (the condition for this is detailed below) then the lower Péclet number limitation for this geometrical regime will come from molecular diffusion.

The cross-over between molecular diffusion and the geometrical dispersion regimes can be obtained by noting that the axial diffusion will contribute to a widening of the tracer cloud, which can readily be obtained from a mere convolution of the geometric transit times by a Gaussian spreading (for small perturbation of the flow, i.e. no stagnation points). Thus, the dispersion coefficients are simply additive and thus a cross-over condition is obtained by balancing the two terms  $D_{\text{G}} = D_{\text{m}}$  or

$$\text{Pe}_{\text{mG}} = \frac{h}{\xi_{\parallel} \varepsilon^2}. \quad (9)$$

Comparing Equations (8) and (9), geometrical dispersion can only exist for

$$\left( \frac{\delta U}{U} \right)^2 = \varepsilon^2 \gg \frac{h}{\xi_{\parallel}}, \quad (10)$$

i.e. large inhomogeneities or large correlation lengths (besides much larger than  $h$  so that the local Poiseuille flow approximation remains valid). Figure 1 summarizes the Péclet dependence of  $D/D_{\text{m}}$  and cross-over scales.

### 2.3. ANOMALOUS DISPERSION REGIME

The rich variety of behaviors encountered in this apparently simple problem is however not exhausted yet. Long-range correlation of the velocity field could result in another ‘anomalous’ regime. Numerous works have shown, using a renormalization group approach, that velocity field correlated over a long range could produce non-diffusive macroscopic dispersion at very small Péclet number [10–13]. However, these works were developed in the limit of vanishing mean velocity, with non-vanishing velocity fluctuations. They do not apply here, because of the proportionality between mean velocity and fluctuations.

Another possible origin of anomalous diffusion, reported some time ago by Mathéron and Marsily [14], is a stratified flow which displays a ‘hyper-diffusive’ behavior. Here, a simple scaling argument due to Bouchaud and George [15] is reproduced. The velocities are assumed to be slowly variable along each streamline as compared to the velocity fluctuations observed in the direction perpendicular to the streamlines. This may be due to a highly anisotropic modulation of the permeability, producing a strong channelling of the flow. In this case, the diffusive motion across the streamlines

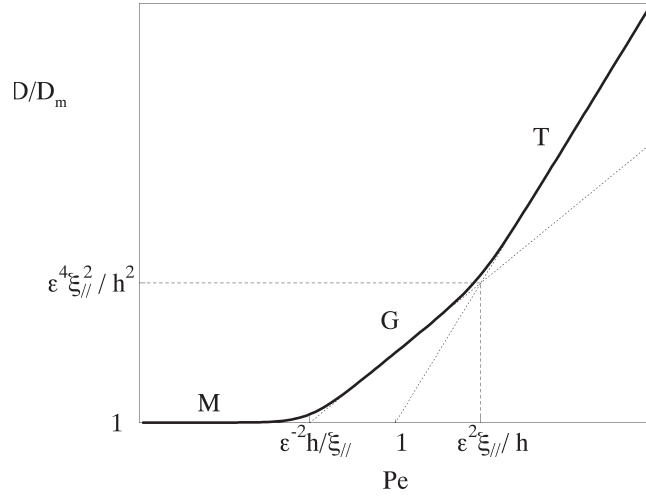


Figure 1. Schematic log–log plot of the dispersion coefficient as a function of the Péclet number based on the mean aperture. The letters **M**, **G** and **T** refer to ‘Molecular’, ‘Geometric’ and ‘Taylor’ regimes respectively, where the slope of the curve is 0, 1 and finally 2. The cross-over Péclet numbers and dispersion coefficients are indicated with notations introduced in the text.

will induce a longitudinal dispersion along the flow due to the difference of velocity between the streamlines.  $\delta U$  still denotes the amplitude of the velocity fluctuation and  $\varepsilon = (\delta U)/U$ . Let  $\xi_{\perp}$  be the *transverse* correlation length of the velocity. The time needed to diffuse perpendicular to the flow direction is  $\Delta t = \xi_{\perp}^2/D_m$ . After a time  $t$  larger than  $\Delta t$ , the tracers will have sampled  $n = \sqrt{t/\Delta t}$  independent streamlines, thus spending roughly  $\sqrt{t\Delta t}$  time units in each streamline. The fluctuating part of the distance travelled in each streamline is of order  $(\delta U)\sqrt{t\Delta t}$ . A sum over  $n$  such independent random distances is needed to obtain a final spreading which amounts to  $(\delta U)\sqrt{t\Delta t}\sqrt{n}$ . Bringing all pieces together, the longitudinal spreading of a tracer spot after a time  $t$  can be written as

$$\Delta x = \varepsilon U \left( \frac{\xi_{\perp}^2}{D_m} \right)^{1/4} t^{3/4}. \quad (11)$$

This spreading is not proportional to  $\sqrt{t}$ , hence the term *anomalous dispersion* to characterize this regime. It is thus not possible to define a dispersion coefficient independent of time or length.

In order to fully understand this regime, it is necessary to explicit its limits. The anomalous dispersion law comes from the fact that the transverse tracer motion samples a small number of channels or streamlines, and each visited channel will induce a much wider spreading. This effect may only be effective if the velocity in one streamline is actually constant. If the longitudinal velocity fluctuation along a distance  $\xi_{\parallel}$  is restored, the anomalous dispersion holds only for times smaller than the time needed to be convected over  $\xi_{\parallel}$ , i.e.  $t^* = \xi_{\parallel}/U$  (assuming small relative

fluctuations of velocities). Thus, at this upper time limit, the spreading is equal to  $\sqrt{Dt^*}$ , which allows to define the dispersion coefficient observed for times longer than  $t^*$ , the expression of which is

$$D = \left( \frac{\delta U}{U} \right)^2 \left( \frac{\xi_{\perp} \xi_{\parallel}^{1/2} U^{3/2}}{D_m^{1/2}} \right). \quad (12)$$

In a dimensionless form, using the Péclet number constructed with the mean aperture of the cell,

$$\frac{D}{D_m} = \varepsilon^2 \left( \frac{\xi_{\perp} \xi_{\parallel}^{1/2}}{h^{3/2}} \right) \text{Pe}^{3/2} \quad (13)$$

and hence a Péclet dependence for this regime which is intermediate between the geometrical  $\mathcal{O}(\text{Pe})$  and Taylor  $\mathcal{O}(\text{Pe}^2)$  dispersions.

The necessary condition for observing this regime is that the transverse diffusion time  $\xi_{\perp}^2/D_m$  be smaller than the longitudinal convection time  $\xi_{\parallel}/U$ . Therefore, the cross-over from anomalous to geometric dispersion occurs for

$$\text{Pe}_{\text{AG}} = \frac{h \xi_{\parallel}}{\xi_{\perp}^2}. \quad (14)$$

The lower limitation comes from a competition with molecular diffusion. Equating both dispersion coefficient provides the cross-over Pe:

$$\text{Pe}_{\text{mA}} = \varepsilon^{-4/3} \frac{h}{(\xi_{\perp}^2 \xi_{\parallel})^{1/3}}. \quad (15)$$

Figure 2 shows the typical evolution of the dispersion coefficient with the Péclet number in a case where the anomalous regime can be seen.

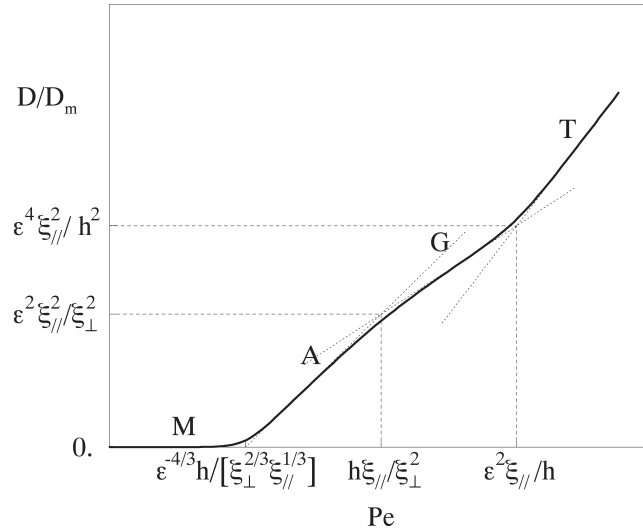


Figure 2. Same as Figure 1, with the anomalous (label A) regime included, with a 3/2 slope.



It should be noted that the limiting process which was assumed to be the anomalous regime was, in fact, the geometrical dispersion regime. It could also be supposed that the Taylor regime could be the limiting process. This case imposes that the upper time limit for the anomalous regime is given by the molecular diffusion time over a distance  $h$ . This however would necessitate that  $\xi_{\perp} \ll h$ , a condition that can never be fulfilled (otherwise the flow problem is three-dimensional, and thus this entire discussion does not justify). Thus, it is concluded that a cross-over from anomalous to Taylor dispersion is unphysical.

To conclude this subsection, the condition for which anomalous dispersion occurs has to be specified. This condition has the simple following form

$$\varepsilon \gg \frac{\xi_{\perp}}{\xi_{\parallel}}, \quad (16)$$

since  $\varepsilon \ll 1$ , this condition imposes that the velocity correlation is extremely anisotropic  $\xi_{\perp} \ll \xi_{\parallel}$ . In particular, for an isotropic correlation, it is impossible to observe the anomalous dispersion regime. An alternative possibility, not explored here, is that the diffusion tensor itself is highly anisotropic. However, in order to observe an anomalous regime in the case where  $\xi_{\perp} = \xi_{\parallel}$ , one requires  $D_{\perp} \gg D_{\parallel}$ , which is a rather unusual situation.

### 3. Geometrical Dispersion in Cracks

Let us extend the previous analysis to the case of heterogeneities which are closer to reality, with applications to flow in open cracks. Dispersion in such structures has already been investigated numerically [5, 16]. The geometrical dispersion regime is examined here theoretically within our model for the aperture geometry.

It has been shown (see [17] for a recent review) that the crack surface  $z(x, y)$  can be accurately described as a *self-affine topography*. The latter is such that the surface roughness obeys (statistically) to a scale invariance which stems from the absence of characteristic length scales. Thus, for any scale factors  $\lambda$ , the height difference  $[z(x + \lambda\delta x) - z(x)]$  has the same statistical features as  $\mu(\lambda)[z(x + \delta x) - z(x)]$ . The scale factor along the  $z$ -axis  $\mu$  is a function of the scale factor  $\lambda$  along  $x$ . Combining two such scale transformations, the identity  $\mu(\lambda_1)\mu(\lambda_2) = \mu(\lambda_1\lambda_2)$  implies that  $\mu$  is a homogeneous function of  $\lambda$ :  $\mu = \lambda^{\zeta}$  where  $\zeta$ , the Hurst or roughness exponent, characterizes a class of such scale-invariant topographies. It is to be noted that such surfaces have long-range spatial correlations. As a consequence of the above symmetry, the standard deviation of the height distribution  $z(x)$  estimated over an interval  $[x, x + \delta x]$  is proportional to  $(\delta x)^{\zeta}$  and thus depends explicitly on the span  $\delta x$ . For crack surfaces, the self-affinity is often observed over a large range of scales [12]. Moreover, a large number of experimental determinations [18–20] of the roughness exponent in rocks fall in a narrow interval of values around  $\zeta \approx 0.8$ . Figure 3 shows the geometry of the considered crack with a synthetic random self-affine surface with a roughness exponent  $\zeta = 0.8$ .

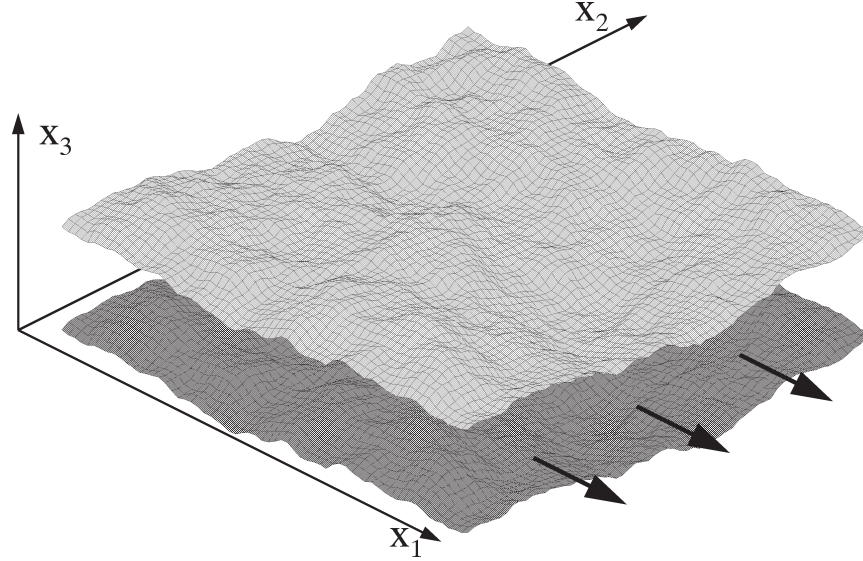


Figure 3. Illustration of the crack geometry considered in this study. The two crack faces are conjugated and translated with respect to each other. The crack surface is self-affine as observed experimentally. Flow takes place as shown with bold arrows.

A flow between the two opposite faces of a crack is considered, and thus the local aperture  $a(x)$  is introduced such that

$$a(x) = h + z(x) - z(x + d), \quad (17)$$

where  $d$  is the in-plane relative shift of the two faces, and  $h$  is the mean aperture of the crack.  $h$  cannot assume any value. It has to be larger than a minimum value  $h_{\min}$  such that the faces have exactly one contact point. In the following, it is assumed that  $h > h_{\min}$  and, hence,  $a(x) > 0$  everywhere.

The covariance of the aperture can be obtained exactly [21] for a self-affine surface, and is given by the following expression for two points separated by  $\mathbf{x}$ :

$$\text{Cov}(\mathbf{x}) = \frac{|\mathbf{d} + \mathbf{x}|^{2\zeta} + |\mathbf{d} - \mathbf{x}|^{2\zeta} - 2|\mathbf{x}|^{2\zeta}}{2|\mathbf{d}|^{2\zeta}}. \quad (18)$$

From the previous formula, two distinct scaling regimes appear. For distances smaller than the shift, the aperture is a self-affine function of exponent  $\zeta$ , whereas, for larger distances, the covariance of the aperture decreases with the distance as

$$\text{Cov}(\mathbf{x}) \sim \zeta \left[ 1 + 2(\zeta - 1) \left( \frac{\mathbf{x} \cdot \mathbf{d}}{|\mathbf{x}| |\mathbf{d}|} \right)^2 \right] \left( \frac{|\mathbf{x}|}{|\mathbf{d}|} \right)^{-2(1-\zeta)}. \quad (19)$$

The relative shift of the two surfaces thus appears to be an intrinsic scale in the aperture which might have been guessed to play a similar role as  $\xi$  in the previous analysis. It will be shown in the following that it is not the case. The key reason for this

difference is the long-range correlation of the velocity field induced by the structure of the aperture. Previous studies proposed to relate an anomalous dispersion regime in fractured rocks to long range correlated velocity field [22, 23] for high Péclet number regime. In the following, such velocity correlation results from the crack surface topography and the joint geometry and, hence, the anomalous dispersion regime will be the consequence of such geometrical effects.

Our analysis is first briefly introduced in the next section using a scaling approach and a simple description of the phenomenon at play, whereas the following section presents a more detailed mathematical presentation of the same phenomenon.

### 3.1. SCALING ARGUMENT

The fluctuation in aperture will modify locally the flow, and to first order in the relative aperture fluctuation  $\delta a/h$ , the velocity is given by

$$v = v^{(0)}[1 + \Gamma * (3\delta a/h)], \quad (20)$$

where  $v^{(0)}$  is the mean velocity for an aperture  $a$ ,  $\Gamma$  is the dipolar Green function of the Laplacian operator, scaling as  $1/r^2$  with the distance, and  $*$  denotes a convolution. A minor factor, linear in  $\delta a$ , coming from the translation of the flux in terms of local velocity, is neglected. Next subsection provides a cleaner derivation of  $v$ . Nevertheless the scaling properties of this equation are preserved.

The time needed to travel a distance  $L_1$  along the flow (direction  $x_1$ ) scales, to first order in  $\delta a/h$ , as

$$T = \frac{L_1}{v^{(0)}} \left( 1 - \frac{3}{h} \int_0^{L_1} \Gamma * \delta a \, dx_1 \right). \quad (21)$$

The integral in the right-hand side has now to be estimated. For a shift  $d$  much smaller than the integration distance  $L_1$ , using the expression of  $\delta a = z(x) - z(x + d)$  and the  $r^{-2}$  behavior of  $\Gamma$  can be used to obtain

$$\begin{aligned} \int_0^{L_1} \Gamma * \delta a \, dx_1 &\approx \int_0^{L_1} \mathbf{d} \cdot \nabla \Gamma * z \, dx_1 \\ &\propto \frac{dL_1^\zeta}{L_1}. \end{aligned} \quad (22)$$

Thus, the fluctuation  $\Delta T = (T - \langle T \rangle)$  of transit time over  $L_1$  is

$$\Delta T \propto \frac{dL_1^\zeta}{hv^{(0)}}. \quad (23)$$

Repeating the argument used in the geometric dispersion section, leads to the determination of the dispersion coefficient,  $D$ , through  $D = L_1 v^{(0)} (\Delta T/T)^2$ :

$$D \propto \frac{v^{(0)} d^2 L_1^{2\zeta-1}}{h^2}. \quad (24)$$

The important scaling is obtained from Equation (22), and the following section is aimed at providing a more detailed justification of it. The above key result of Equation (24) will be discussed at the end of the next section.

### 3.2. DETAILED COMPUTATION

The most important object to deal with in the analysis of tracer dispersion is the velocity field. To obtain it from the aperture map, it is proposed here a simple first-order perturbation analysis. Several preceding works have extensively used such weak disorder expansion approach in the context of tri-dimensional heterogeneous porous media in direct space [24, 25] or in Fourier space [9]. A particularity of the crack geometry is that the flux is conserved, and hence the velocity field is not divergence free. This will necessitate, a specific treatment, albeit close to [9].

Our analysis is based on two important restrictions:

- It is assumed that slopes are small,  $|\nabla a| \ll 1$  so that locally a Poiseuille flow in the aperture direction can be used, i.e. Reynolds or ‘lubrication’ approximation.
- Only small deviations from the constant aperture are considered, i.e.  $\delta a(x) = (a(x) - h) \ll h$ .

The Reynolds approximation allows to relate the (aperture-averaged) velocity field in the crack to the pressure gradient,  $\nabla P$ , as

$$\mathbf{v}(x) = -\frac{a(x)^2}{12\eta} \nabla P, \quad (25)$$

where  $\eta$  is the fluid viscosity. The total fluid flux at a point is the velocity times the aperture and, hence, fluid incompressibility imposes

$$\nabla \cdot (a(x)\mathbf{v}(x)) = 0 \quad (26)$$

so that,

$$\nabla \cdot (a(x)^3 \nabla P) = 0. \quad (27)$$

A perturbation computation of the velocity field, in the small parameter  $\varepsilon = (\delta a/h)$  is proposed. All quantities like the pressure  $P$  are expanded as  $P = P^{(0)} + \varepsilon P^{(1)} + \varepsilon^2 P^{(2)} \dots$ . The zeroth-order solution (i.e.  $a(x) = h$ ) gives for an imposed pressure gradient ( $\nabla P^{(0)}$ ):

$$\mathbf{v}^{(0)}(x) = -\frac{h^2}{12\eta} (\nabla P^{(0)}). \quad (28)$$

The first-order correction is obtained through the identification of all terms of order  $\varepsilon$ . The first correction to pressure is such that

$$\nabla^2 P^{(1)} = -\frac{3}{h} \nabla \delta a \cdot \nabla P^{(0)}. \quad (29)$$

Hence, in Fourier space, (Fourier transforms are denoted by a superscript tilde,  $\mathbf{k}$  is conjugated to  $\mathbf{x}$ , and  $k$  denotes its norm,  $k^2 = \mathbf{k} \cdot \mathbf{k}$ )

$$\widetilde{\nabla P}^{(1)} = -3 \frac{\widetilde{a(k)}}{h} \frac{\mathbf{k}(\mathbf{k} \cdot \nabla P^{(0)})}{k^2}. \quad (30)$$

Since  $a$  and  $\delta a$  only differ by a constant  $h$ ,  $\widetilde{a}$  can be substituted to  $\widetilde{\delta a}$  as long as  $k \neq 0$ . The first-order velocity term,  $v^{(1)}$ , is

$$\mathbf{v}^{(1)} = -\frac{2h\delta a}{12\eta} (\nabla P^{(0)}) - \frac{h^2}{12\eta} (\nabla P^{(1)}) \quad (31)$$

which in Fourier space gives

$$\widetilde{\mathbf{v}}^{(1)} = |\mathbf{v}^{(0)}| \frac{\widetilde{a(k)}}{h} \left[ 3 \frac{\mathbf{k}(\mathbf{k} \cdot \mathbf{e}_1)}{k^2} - 2\mathbf{e}_1 \right], \quad (32)$$

where  $\mathbf{e}_1$  is a unit vector along the flow direction. The latter rewriting shows that  $v^{(1)}$  is proportional to  $v^{(0)}$  and of order 1 in  $\varepsilon$ .

In this geometry, the molecular diffusion and Taylor regimes are trivially recovered at, respectively, very low and high Pe numbers. The anomalous dispersion regime cannot be observed since the geometry is not stratified along the flow. Thus, the only regime of interest is the geometric dispersion. When  $\text{Pe} < 1$ , the actual advection velocity is the aperture-averaged velocity, i.e. the two-dimensional field considered in the present section. In order to estimate the dispersion coefficient, advection of the tracer along the two-dimensional flow only has to be considered.

For convenience of the analysis, a line of tracer launched in the flow along the  $x_1 = 0$  line at time  $t = 0$  is considered, and the arrival time  $T(L_1, x_2)$  after a prescribed convection distance  $L_1$  is studied. The crack surface will conveniently be generated in Fourier space, and  $L$  denotes its size. Not to be restricted by the boundary conditions or the periodicity of the system, only  $L_1 \ll L$  is considered. The arrival time amounts to (first-order in  $\varepsilon$ )

$$T(L_1, x_2) = \frac{1}{|v^{(0)}|} \left( L_1 - \int_0^{L_1} \frac{\mathbf{v}^{(1)} \cdot \mathbf{e}_1}{|v^{(0)}|} dx_1 \right). \quad (33)$$

The latter integral only requires the axial velocity perturbation. This result is, at this approximation order, equivalent to those obtained by various approaches in [9, 26, 27], giving the longitudinal dispersion coefficient in term of a simple integral over the velocity field covariance in the mean flow direction. Let us introduce

$$\phi(L_1, x_2) = \int_0^{L_1} \frac{\mathbf{v}^{(1)} \cdot \mathbf{e}_1}{|v^{(0)}|} dx_1. \quad (34)$$

In order to perform the integration, one should treat separately the  $k_1 = 0$  components of the Fourier transform, since the latter prevents the integral of  $\phi$  from being periodic. The Fourier transform of the periodic part  $\phi_p$  of  $\phi$  is written as

$$\widetilde{\phi}_p = \frac{i}{k_1} \frac{\widetilde{a(k)}}{h} \left( \frac{k_1^2 - 2k_2^2}{k^2} \right), \quad (35)$$

whereas the  $k_1 = 0$  case corresponds in real space to

$$\phi_{\text{np}}(L_1, x_2) \equiv L_1 f(x_2) = -2 \int_0^{L_1} \frac{\delta a(x'_1, x_2)}{h} dx'_1. \quad (36)$$

In most cases, this nonperiodic part can be dropped when  $L$  goes to infinity. It simply reflects a spurious finite size effect. Moreover, since only time differences matter, this contribution will vanish.

The expression of the tracer transit time with its correction to first order in the small parameter  $\varepsilon = \delta a/h$  has been established. This result also assumes  $|\nabla \delta a| \ll 1$ . This result is quite general and not restricted to the particular crack surface topography and aperture of the rock joint model. The above result is now specialized to self-affine crack surfaces.

### 3.2.1. Self-Affine Crack

Let us now use the specific crack geometry considered in this section. The self-affine crack surface  $z$  can conveniently be generated in Fourier space as

$$\tilde{z}(\mathbf{k}) = A|k|^{-1-\zeta} \tilde{\alpha}(\mathbf{k}), \quad (37)$$

where the  $\tilde{\alpha}$  are uncorrelated random complex Gaussian variables of zero mean and unit variance (including usual conjugation properties for  $z$  to be real).  $A$  is a prefactor which sets the absolute roughness at a unit scale. Indeed the mean variance of  $z$  over a domain of size  $L$  is obtained directly from Parseval theorem as

$$\sigma^2(L) \equiv \frac{1}{L^2} \iint_{L \times L} z^2 d^2x \propto A^2 L^{2\zeta} \quad (38)$$

up to numerical prefactors. One important point to note is that the small wavelength cut-off only contributes to a small correction dropped from the above expression.

The aperture fluctuation part is  $\delta a(x) = z(x) - z(x+d)$  which in Fourier space is written

$$\tilde{a} = (1 - e^{i\mathbf{k}\cdot\mathbf{d}}) \tilde{z}. \quad (39)$$

At large wavelengths  $\mathbf{k} \cdot \mathbf{d} \ll 1$ , a Taylor expansion of the exponential gives  $\tilde{a} = -i(\mathbf{k} \cdot \mathbf{d}) \tilde{z}$ , i.e. the gradient of  $z$  in the  $d$  direction times  $d$ . This allows us to retrieve simply the large-scale behavior of the covariance of the aperture, which can be seen as a self-affine field of exponent  $\zeta - 1 < 0$ . As a side remark, an interesting analogy can be drawn between the aperture field and a dipolar effect.

All the necessary ingredients to analyze the scaling features of the transit times in a crack are now available. The expression of  $a$  in the equation giving the function  $\phi$  is now used to arrive at the following scaling behavior for long wavelength  $\mathbf{k} \cdot \mathbf{d} \ll 1$ :

$$\tilde{\phi}_p = \frac{A \mathbf{k} \cdot \mathbf{d}}{h} \frac{|k|^{-1-\zeta} \tilde{\alpha}(\mathbf{k})}{k_1} \left( \frac{k_1^2 - 2k_2^2}{k^2} \right). \quad (40)$$

The nonperiodic part is linear in  $L_1$ , and the Fourier transform along  $x_2$  of its amplitude,  $f$ , has a modulus scaling as  $k_2^{-\zeta}$ ; hence, it is a self-affine profile of exponent  $\zeta - 1/2$  above a scale  $d_2$ . As already mentioned above, this term will only result in a minor (sub-dominant) contribution to  $\phi$ .

The inverse Fourier transform of expression (40) gives the final result as

$$\phi(L_1, x_2) = \phi_p(L_1, x_2) - \phi_p(0, x_2) + L_1 f(x_2). \quad (41)$$

One may also note that, in the particular case where  $\mathbf{d}$  is along the  $x_1$  axis (since the main flow is supposed to occur along  $x_1$ , the relative shift of the crack faces is parallel to the mean flow),  $\tilde{\phi}(0, k_2)$  is identically 0.

The important property to be noted in Equation (40) is the homogeneity of  $\tilde{\phi}_p$  with respect to  $k$ , with a degree  $(-1 - \zeta)$ . This is similar to the Fourier transform of the crack surface  $\tilde{z}$ . It is thus concluded that  $\phi_p$  is *itself a self-affine function characterized by a roughness exponent  $\zeta$* . Although  $\phi$  is markedly anisotropic, the same roughness exponent  $\zeta$  appears along any direction in the  $(x_1, x_2)$  plane. Finally, the Fourier transform of  $\phi$  includes contributions from wavenumbers as low as  $2\pi/L$ , where  $L$  is the system size. However, when performing the difference  $\phi_p(L_1, x_2) - \phi_p(0, x_2)$ , the wavenumber smaller than  $2\pi/L_1$  will be filtered out from the final expression of  $\phi$ . Hence,  $\phi(L_1, x_2)$  considered as a function of  $x_2$  is a self-affine function of exponent  $\zeta$  from the lower cut-off scale up to  $L_1$  (and not  $L$ ). For distances  $\Delta x_2 \gg L_1$ , the expectation value of  $(\phi(L_1, x_2 + \Delta x_2) - \phi(L_1, x_2))^2$  saturates to a value  $A^2 L_1^{2\zeta}$  independent of  $\Delta x_2$ .

Estimating the variance of  $\phi$  (its mean is obviously 0) gives a direct estimate of the fluctuation  $\Delta T$  of the transit time over a scale  $L_1$ :

$$\begin{aligned} \left(\frac{\Delta T}{T}\right)^2 &= \frac{A^2}{h^2 L_1^2} \iint [(\cos(k_1 L_1) - 1)^2 + \sin^2(k_1 L_1)] \times \\ &\quad \times k^{-2-2\zeta} \left(\frac{\mathbf{k} \cdot \mathbf{d}}{k_1}\right)^2 \left(\frac{3k_1^2}{k^2} - 2\right)^2 dk_1 dk_2. \end{aligned} \quad (42)$$

Upon a change of variable, this variance can be recast in a simple form:

$$\left(\frac{\Delta T}{T}\right)^2 = \frac{A^2 L_1^{2\zeta-2}}{h^2} (K_{\parallel}(\zeta) d_1^2 + K_{\perp}(\zeta) d_2^2), \quad (43)$$

where  $K_{\parallel}$  and  $K_{\perp}$  are two definite integrals which only depends on the roughness exponent  $\zeta$ . These two parameters define the dispersion anisotropy induced by the aperture anisotropy of Equation (19). Previous numerical works [29] have studied the influence of fracture surfaces anisotropy on dispersion. It is important to note here that such anisotropy emerges from a direction of translation between two statistically *isotropic* surfaces. To obtain the expression of the dispersion coefficient, the same argument as given in the second section is used to derive

$$D = \frac{v^{(0)} A^2 L_1^{2\zeta-1}}{h^2} (K_{\parallel}(\zeta) d_1^2 + K_{\perp}(\zeta) d_2^2) \quad (44)$$

or introducing the Péclet number scaled on the aperture, and the mean roughness  $\sigma(L_1)$  of the crack surface on the scale  $L_1$ , and ignoring the anisotropy of the dispersion tensor, the following scaling estimate is obtained:

$$\frac{D}{D_m} = \text{Pe} \frac{\sigma(L_1)^2}{hL_1} \frac{d^2}{h^2}. \quad (45)$$

Different properties are worth mentioning at this stage.

- In spite of the nontrivial scaling of the widening of the front with the distance,  $D$  simply remains proportional to the mean velocity, an essential property of the geometric regime. This can be understood from the observation that this regime is purely advective, i.e. independent of the molecular diffusion coefficient, and thus changing the velocity, without changing the front widening after a fixed advected distance.
- Although the aperture is mostly controlled by the roughness estimated at the scale of the shift  $d$ , the front width reveals the roughness of the *crack surface* itself, over much larger scales.
- The dispersion coefficient is a rough characterization of the dispersion process. From the previously determined  $\phi$  function, a more detailed description of the tracer distribution can be dealt with. The computation is done in an equivalent infinite two-dimensional Péclet number, since molecular diffusion does not play any role. In fact, it can be shown that the line of tracer will become distorted as time evolves, and it will finally acquire a self-affine geometry reminiscent of the vertical topography of one crack face. The roughness of the front is self-affine with an exponent  $\zeta$ , and its upper wavelength is in a first transient regime proportional to the travelled distance. Larger wavelengths do not have enough time to be revealed by the flow. For a persistent geometry,  $\zeta > 1/2$  – the usual case for cracks where  $\zeta \approx 0.8$  – the width of the front, proportional to  $L^\zeta$  corresponds to an apparently *hyperdiffusive* process. In addition to the roughening of the tracer front, the following section shows that the front itself widens, in a way which can again be characterized extensively.
- The shift of the two crack faces  $d$  plays a significant role in the dispersion coefficient. The fact that the latter vanishes in the limit of a zero shift comes from the fact that our analysis is restricted to the first order in  $\nabla a$  and, thus, the aperture becomes constant for a simple vertical translation of the crack faces. In fact the flow is affected by such a shift but only to second order in  $\nabla a$ .

### 3.3. INTRINSIC WIDENING OF THE TRACER LINE

Above, the scaling of the dispersion estimated from the meandering of the tracer line due to velocity fluctuations has been obtained. The tracer not along an entire line perpendicular to the flow, but rather at a particular point can be characterized. Then the previous treatment is inadequate for giving information on the measured



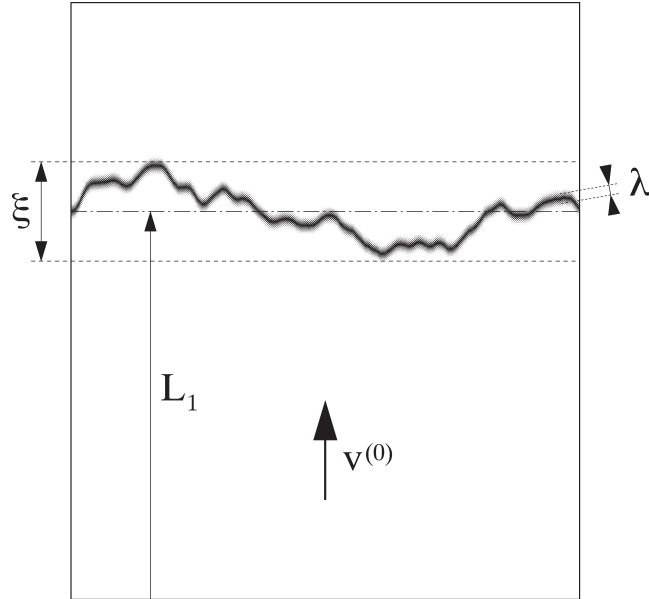


Figure 4. Schematic representation of the tracer curve after a finite time of advection. The wrinkling of the curve over the scale  $\xi$  gives rise to a large dispersion coefficient which is important for the global tracer distribution. However, a point measurement is unable to capture this global quantity, but is rather sensitive to the ‘intrinsic widening’ of the tracer locus (scale  $\lambda$  in the figure). These two processes are analysed respectively in Sections 3 and 4.

signal. The previously computed dispersion coefficient would provide the point-to-point fluctuation of the mean transit time, thus, it is relevant for analyzing the statistics of an ensemble of such measurements. Locally, a point detector would see a tracer spreading much smaller than the one estimated from formula (45). This effect, illustrated in Figure 4, is analyzed in the present section.

Different effects may contribute to this intrinsic widening. Focusing on a single streamline, the molecular diffusion along the flow direction  $x_1$  will provide a dispersion mechanism which plays a role only at very small Péclet numbers. Tracer diffusion along the aperture direction  $x_3$  will induce a Taylor dispersion mechanism, if the Péclet number is large enough. These two cases are essentially similar to the case discussed in the second section of this paper. The most interesting case is the one where diffusion may occur along  $x_2$  perpendicular to the streamline, but in the mean crack plane. Indeed, following the streamline, a close analogy with the stratified flow case can be drawn and, thus, it may be expected that an anomalous dispersion mechanism will take place, contributing to the ‘intrinsic’ widening of the tracer around its mean locus.

A fixed advected distance equal to  $L_1$  is considered. Molecular diffusion will allow the tracer to explore a distance perpendicular to the flow lines of order  $\Delta x_2 = (D_m T)^{1/2}$ . One difference with the stratified flow case as analyzed previously

(Section 2) is that now the velocity is not constant along the streamlines. However, the advection time difference between flow lines can be treated as roughly independent from  $x_1$  since the longest wavelengths of the aperture fluctuation contribute dominantly to the advection, and thus the wavelengths smaller than the entire trajectory play only a minor role. Another (more important) difference is the existence of long-range correlations in the aperture field. However, the previous analysis has revealed all the necessary information to proceed. Indeed, the tracer locus lies on a self-affine curve of exponent  $\zeta$ , and thus the difference in transit time for two points at a distance  $x_2$  perpendicular to the flow scales as  $\Delta T \propto x_2^\zeta$  as long as  $x_2 \ll L_1$ . (More precisely,  $\Delta T(x_2) = (Ax_2^\zeta d)/(v^{(0)}h)$ .) From this estimate, the difference in mean velocity along the streamlines is deduced.

All the material is now at hand to conclude. The widening of the tracer locus amounts to

$$\Delta x_1 \propto \frac{Ad (D_m T)^{\zeta/2}}{h}. \quad (46)$$

This expression is now used to define the ‘local’ dispersion coefficient  $D_1$  through  $\Delta x_1 \equiv (D_1 T)^{1/2}$ . Hence,

$$D_1 = \frac{A^2 d^2 D_m^\zeta (v^{(0)})^{1-\zeta}}{h^2 L_1^{1-\zeta}}. \quad (47)$$

Which can be rewritten in dimensionless form as

$$\frac{D_1}{D_m} = \frac{A^2 d^2}{h^2} \left( \frac{\text{Pe}}{h L_1} \right)^{1-\zeta} = \frac{d^2}{h^2} \frac{\sigma(h)\sigma(L_1)}{h L_1} \text{Pe}^{1-\zeta}. \quad (48)$$

It is also instructive to express the ratio of the local dispersion coefficient  $D_1$  to the global one,  $D$ , computed in the preceding section:

$$\frac{D_1}{D} = \left( \frac{L_1 \text{Pe}}{h} \right)^{-\zeta}. \quad (49)$$

From these last expressions, which constitute the second key result of this paper, it is noted that

- The local dispersion coefficient is much smaller than the global dispersion coefficient obtained previously, as long as the diffusion distance is much smaller than  $L_1$ . This justifies the qualitative picture of Figure (4).
- The local dispersion coefficient displays an anomalous dependence on the Péclet number as a power law with an exponent  $(1 - \zeta)$ . In the case of cracks, using  $\zeta = 0.8$ , the velocity dependence of the dispersion coefficient is weak.
- The relative shift  $(d/h)$  appears quadratically in the expression for  $D_1$  as already seen for the expression of the global dispersion coefficient  $D$ .

- The surface roughness appears both at the aperture scale  $h$  and at the advection scale  $L_1$  in Equation (48). This may appear as surprising but simply results from the choice of introducing the Péclet number based on the crack aperture  $h$ . A different (and legitimate) choice consists in using  $L_1$  instead of  $h$ ,  $\text{Pe}^* = v^{(0)} L_1 / D_m$ . This would turn the previous expression into

$$\frac{D_1}{D_m} = \frac{d^2}{h^2} \frac{\sigma(L_1)^2}{L_1^2} \text{Pe}^{*1-\zeta}, \quad (50)$$

i.e. the same prefactor to the  $\text{Pe}^*$  number as for the global dispersion coefficient.

- Similarly, the ratio of the local to global dispersion coefficient takes the simple form

$$\frac{D_1}{D} = \text{Pe}^{*-\zeta}. \quad (51)$$

- Finally, a possible way to reveal the local dispersion mechanism is to perform ‘echo’ experiments [6] where the flow is reversed after some period of time, as done numerically in [28]. In this case, the geometric dispersion is erased and the ‘intrinsic widening’ of the tracer line is the major source of dispersion. An anomalous dispersion coefficient similar to  $D_1$  with  $L_1$  equal to the mean convected distance at the point of flow reversal is expected.

#### 4. Conclusion

After having recalled the scaling features of the dispersion mechanisms in an imperfect Hele-Shaw cell, a realistic open crack geometry has been taken into account, with the multiple scale surface topography, for the only regime (geometric dispersion) which is controlled by the large-scale flow inhomogeneities. Using a perturbation expansion up to first order, the expression of the dispersion coefficients have been developed either for global or local measurements. These coefficients are shown to depend on the global roughness of a crack face, on the mean aperture and on the relative shift between the crack faces. Finally, the Péclet dependence of both types of measurements has been shown to be dramatically different.

The importance of this final result is now emphasized. In contrast to laboratory-scale experiments which most naturally focus on global measurements, field measurements are much easier to perform through local measurements of the tracer concentration in a narrow region. It is thus essential to be able to bridge up both determinations. Large-scale features of the crack surface, which are mostly wiped out from the aperture field, do reappear in dispersion problems. In particular, they give rise to a dramatic difference between local and global dispersion properties.

## Acknowledgements

Useful discussions with E. J. Hinch are gratefully acknowledged. This study has been partly supported by the ECOTECH program and the Groupement de Recherche CNRS 1025 ‘Physique des Milieux Hétérogènes Complexes’.

## References

1. Taylor, G. I.: Dispersion of solute matter in solvent flowing slowly through a tube, *Proc. Roy. Soc. London A* **219** (1953), 186.
2. Aris, R.: On the dispersion of a solute in a fluid flowing through a tube, *Proc. Roy. Soc. London A* **235** (1956), 65–77.
3. Koplik, J., Ippolito, I. and Hulin, J. P.: Tracer dispersion in rough channels: a two dimensional numerical study, *Phys. Fluid* **A5** (1993), 1333.
4. Gutfraind, R., Ippolito, I. and Hansen, A.: Study of tracer dispersion in self-affine fractures using lattice-gas automata, *Phys. Fluids* **7**(8) (1995), 1938–1948.
5. Thompson, M. E.: Numerical simulation of solute transport in rough fractures, *J. Geophys. Res.* **96**(B3) (1991), 4147–4166.
6. Ippolito, I., Daccord, G., Hinch, E. J. and Hulin, J. P.: Echo tracer dispersion in model fractures with a rectangular geometry, *J. Contam. Hydrol* **16**(2) (1994), 87–108.
7. Golay, M. J. E.: in: D. H. Destye (ed.), *Gas Chromatography*, Butterworths, London, 1958, pp. 36–52.
8. Matheron, G.: *Eléments pour une théorie des milieux poreux*, Ed. Masson, Paris, 1967.
9. Gelhar, L. W. and Axness, C. L.: Three-dimensional stochastic analysis of macrodispersion in aquifers, *Water Resour. Res.* **19**(1) (1983), 161–180.
10. Gevorkian, Zh. S. and Lozovik, Y. E.: Classical diffusion in random fields with long-range correlations, *J. Phys. A* **20** (1987), L659.
11. Aronovitz, J. A. and Nelson, D. R.: Anomalous diffusion in steady fluid flow through a porous medium, *Phys. Rev. A* **30**(4) (1984), 1948.
12. Bouchaud, J. P. and George, A.: Anomalous diffusion in disordered media: statistical mechanisms, models and physical applications, *Phys. Rep.* **195** (1990), 128–293.
13. Glimm, J. and Sharp, D. H.: A random field model for anomalous diffusion in heterogeneous porous media, *J. Stat. Phys.* **62**(1–2) (1992), 415–424.
14. Matheron, G. and Marsily, G.: Is transport in porous media always diffusive? A counterexample, *Water Resour. Res.* **16** (1980), 901.
15. Bouchaud, J. P. and George, A.: Simple model for hydrodynamic dispersion, *C. R. Acad. Sci. II* **307** (12) (1988), 1431–1436.
16. Grindrod, P. and Impey, M.: Channeling and Fickian dispersion in fractal simulated media, *Water Resour. Res.* **29**(12) (1993), 4077–4089.
17. Bouchaud, E.: Scaling properties of cracks, *J. Phys. Condens. Matter* **9** (1997), 4319–4344.
18. Brown, S. R.: A note on the description of surface roughness using fractal dimension, *Geophys. Res. Letter* **14** (1987), 1095–1098.
19. Poon, C. Y., Sayles, R. S. and Jones, T. A.: Surface measurement and fractal characterisation of naturally fractured rocks, *J. Phys. D: Appl. Phys.* **25** (1992), 1269–1275.
20. Schmittbuhl, J., Gentier, S. and Roux, S.: Field measurements of the roughness of fault surfaces, *Geophys. Res. Lett.* **20** (1993), 639.
21. Plouraboué, F., Kurowski, P., Hulin, J. P., Roux, S. and Schmittbuhl, J.: Aperture of rough cracks, *Phys. Rev. E* **51**(3) (1995), 1675.
22. Neuman, S. P.: On advective transport in fractal permeability and velocity fields, *Water Resour. Res.* **31**(6) (1995), 1455–1460.

23. Berkowitz, B. and Scher, H.: On characterization of anomalous dispersion in porous and fractured media, *Water Resour. Res.* **31**(6) (1995), 1461–1466.
24. Dagan, G.: Solute transport in heterogeneous porous formation, *J. Fluid Mech.* **145** (1984), 151–177.
25. Dagan, G.: Theory of solute transport by groundwater, *Ann. Rev. Fluid Mech.* **19** (1987), 183–215.
26. Avallaneda, M. and Majda, A. J.: Renormalization theory for eddy diffusivity in turbulent transport, *Phys. Rev. Lett.* **68** (1992), 3028–3031.
27. Glimm, J., Lindquist, W. B., Pereira, F. and Zhang, Q.: A theory of macrodispersion for the scale up problem, *Transport in Porous Media* **13** (1993), 97–122.
28. Flekkøy, E. G.: Symmetry and focussing in mixing Fluids, to appear in *Phys. Rev. Lett.* (1997).
29. Thompson, M. E. and Brown, S. R.: The effect of anisotropic surface roughness on flow and transport in fractures, *J. Geophys. Res.* **96**(B13) (1991), 21923–21932.